Corona discharge photography

David G. Boyers and William A. Tiller

Department of Materials Science and Engineering, Stanford University, Stanford, California 94305
(Received 17 January 1973)

Using short ($\sim$100 μsec) pulses of rf (1 MHZ) applied to parallel electrodes in air at small electrode spacings ($\sim$ 250 μ) and at an applied field of $\sim 10^6$ V/cm, discharges from both biological and metallic electrodes occurred from a network of points in the electrode surface. These discharges were recorded photographically. Multiple pulses lead to a superposition effect such that a uniform corona exposure appeared on the film. Some effects of electrode material, spacing, and orientation are presented. The results are found to be completely explicable in terms of the "streamer" phenomenon of corona discharge. In fact, the wide variety of color effects observed in "Kirlian" photography can be accounted for by this mechanism.

I. INTRODUCTION

In recent years considerable interest has developed in a type of high-voltage photography called Kirlian photography after its chief developer, Semyon Kirlian, who investigated many aspects of the technique over a 30-year period.[1,2] A review of some of the Soviet work and some English work has been given recently by one of the authors,[2] so no extended discussion of this work will be given here.

Current interest in this subject is very high on the part of psychologists, psychiatrists, and biologists who look upon the technique as a unique way of observing energy fields associated with all living things. Extravagant claims are being made about the process based upon very little information. Of course, the fascinating color photographs of plant leaves and human fingertips[3] would make anyone wax poetic (see Fig. 1). On the one hand, the intensity and character of the energy emissions seem to depend strongly on the mental, emotional, and physical health condition of the subject being photographed, and this has prompted some people to postulate new types of energy emission from the body (called bioplasmic energy by the Soviets). On the other hand, the process itself is clearly associated with an electrical discharge and looks, on the surface, like a corona discharge effect[4] which has prompted other people to relegate the entire phenomenon to a category of fairly familiar electrical-discharge effects. Of course, both viewpoints may be correct in part; i.e., new energy forms embodying information about the living system may be manifest within the context and framework of the electrical-discharge phenomenon.

To sort out this controversy will require careful experimantation under well-controlled conditions leading to completely reproducible results. Such a condition does not presently exist, so the authors decided to embark upon such a program and chose, after an initial learning period during which some of the Soviet work was reproduced, to start by investigating discharge patterns between flat polished metallic electrodes rather than going directly to living systems. The first part of the paper deals with the equipment, design, and the reproduction of some Soviet work. The second part deals with new work on steel, brass, and silicon electrodes. In Sec. IV, a simple theory is presented to illustrate how a variety of color effects can be generated without any alteration of state of the material object being used as an electrode.

II. EQUIPMENT

A schematic representation of a simple Soviet device and power-source characteristic is given in Fig. 2. The object to be photographed is placed between the parallel metal plates of a capacitorlike arrangement and separated by a small distance from a piece of photographic film (emulsion side towards the object). The Soviets indicate that a certain critical spacing d be maintained between the object and the film.

A block diagram of our equipment setup is given in Fig. 3. An Oudin coil coupled to the output of a modified radio transmitter was used to generate the high-voltage rf used in our experiments. The pulse width was freely variable, with 100–500 μsec pulses being used most often. The pulse repetition rate was also variable although, usually, a single pulse was used. The rf frequency for these experiments was set at 1 MHz and the output voltage was adjusted to be about 20 kV by altering the turns ratio of the Oudin coil. In our case, the voltage was not unipolar as indicated in Fig. 2 but was bipolar; i.e., equal positive and negative swings. A more detailed discussion of the rf voltage source is given in the Appendix.

Our initial electrode configuration was modeled after that of Kirlian and is illustrated in Fig. 4. With the use of a relatively high rf frequency, $\omega = 2\pi \times 10^6$ rad/sec, the effective load impedance $Z_L = 1/\omega C_L$ would be relatively small for the larger values of load capacitance, $C_L = \epsilon_0 A/d$, due to a large electrode area A and small electrode spacing d. Since the rf transmitter with its Oudin-coil output stage is a nonideal source with a relatively high source impedance, a relatively small load impedance would result in dropping most of the voltage across the source impedance, leaving little voltage applied to the load. This pointed up the need to use a lower frequency for the photographing of plant leaves and other large surface areas. Rather than changing our two resonant circuits and, thus, the rf frequency, we decided to remain at 1 MHz and check our system out on smaller surface areas such as coins and fingertips.

For photographing coins and fingertips, we found it easier to use a single-electrode configuration such as illustrated in Fig. 5. The edges of the copper electrode were rounded in order to reduce the tendency for field emission at the edges.

FIG. 1. Kirlian photograph of leaf (courtesy of Thelma Moss).

For the photographing of coins, a ground wire is necessary; however, for fingertips it is unnecessary because the capacitive coupling at high frequencies effectively grounds the individual. For both cases (in a darkened room under red safelight illumination), a sheet of Kodak 6127 commercial film is placed, emulsion side up, on the copper electrode, and the coin or finger is spaced a small distance from the film. The coin spacing is determined by the relief of the coin surface, since the coin is actually placed in physical contact with the emulsion surface. The minimum fingertip film spacing is set as approximately 5—10 mil. However, because of the curvature of the fingertip, the spacing changes over the fingertip. The rf voltage source was set to give either single or multiple pulses during the time of film exposure.

III. RESULTS

A. Phase I

The results of photographing a coin are illustrated by Fig. 6(a) for multiple pulses and by Fig. 6(b) for a single pulse. We notice that Fig. 6(a) could arise from a superposition of events of the type illustrated by Fig. 6(b), and we also notice the clear delineation of all the sharp edges due to the relief in the coin surface. The latter suggests enhanced field emission of electrons from regions of small radius of curvature.

The results of photographing a fingertip are illustrated in Fig. 6(c) for multiple pulses and are very similar to the results of the Soviet work and that of other investigators.[3] The pattern is essentially halolike and is dif-

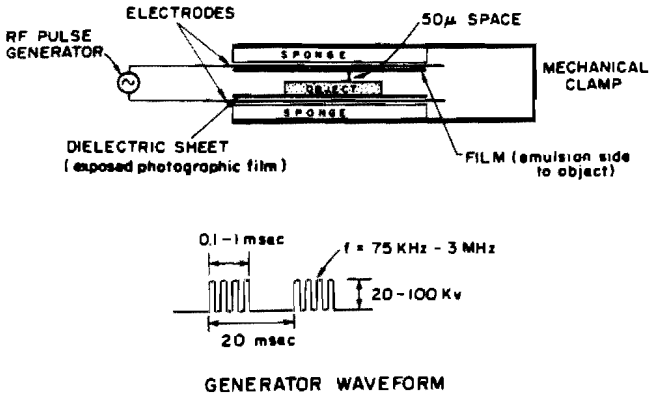

FIG. 2. Simple Kirlian photographic equipment and waveform using capacitor-plate configuration.

fuse in nature. The same finger photographed with a single pulse is shown in Fig. 6(d). Once again, as in the case of the coin, we see a sharply discrete pattern as if emission occurred from a network of points. In Fig. 7 further examples of this discrete emission from fingertips is given. In the center photo of the Fig. 7 composite, we see the result of a somewhat greater discharge spacing. This would seem to have arisen as a result of a decrease in the number of main discharge channels. The figure also shows the diffuse exposure due to uv light and the Clayden photographic effect due to uv light exposing the film just prior to streamer exposure.[4] This figure appears quite similar to the "Lichtenberg" figures taken by Nasser in point-to-plane corona discharge studies.[5]

During the fingertip studies, it was found that the photograph depended significantly on the orientation and spacing of the finger to the electrode-film combination. Variability in these results occurred as a result of the inability to repeatably establish a well-defined and controlled discharge spacing. Obviously, to obtain reliable results, one must control the orientation and spacing of the living electrode from the film. As a step in the direction of developing such techniques, we decided to investigate discharges between identical flat polished metal electrodes.

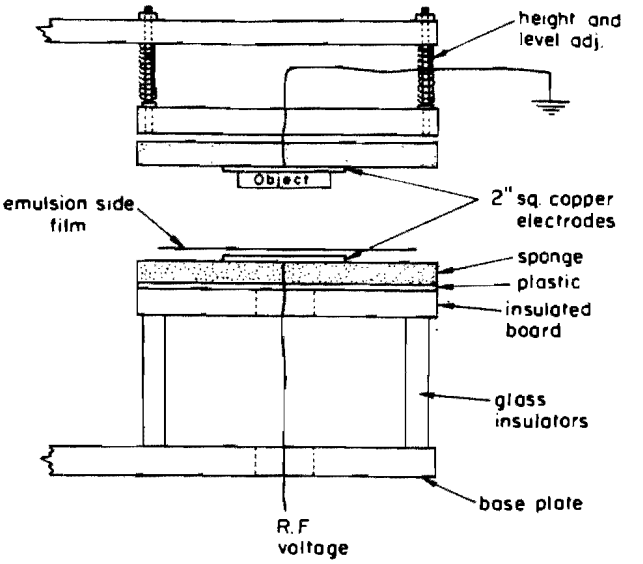

FIG. 4. Initial electrode configuration mounted on an alignment device.

B. Phase II

In this phase of the work, we investigated the discharge between flat polished electrodes in order to have greater control over surface composition, surface topography (gross shape), surface smoothness, interelectrode spacing, and uniformity of spacing (parallelism of electrodes). The character of the discharge photographs seemed to be influenced by all of these factors. The experiments were carried out in air and no special precautions were taken to control water vapor, dust, etc., although all of the work was carried out in an air-conditioned room at ~68 °F. Three different materials were studied—brass, stainless steel, and silicon. The silicon was cut from a semiconductor-grade single crystal, whereas the others were commercial-grade polycrystalline samples. The samples ($\frac{5}{8}$ in. diam and $\frac{3}{4}$ in. long) were mounted in a cylindrical plastic mount ($1\frac{1}{4}$ in. diam) and one face of each was polished to a smoothness of 1 μ on a diamond wheel. The other face was left with a rough polish as the electrical contact surface with the generator. The large copper electrode was replaced by

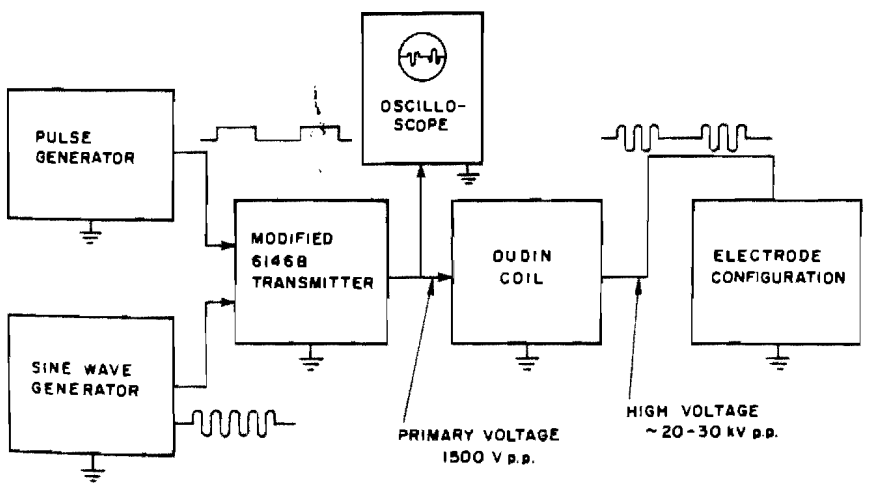

FIG. 3. Block diagram of equipment built by authors.

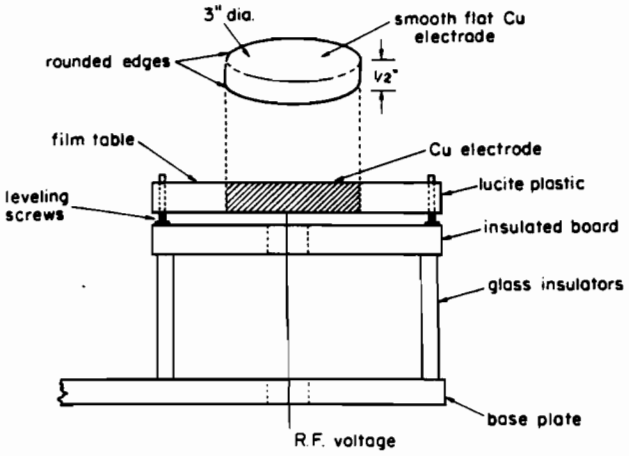

FIG. 5. Single-electrode configuration for photographing fingertips.

a matched $\frac{5}{8}$-in. diam sample electrode. The samples were held in the apparatus illustrated in Fig. 8, which maintained the two electrodes in a parallel arrangement at ~10-mil spacing. The film (4 in. by 5 in.), placed emulsion side up on the film table, was held relatively flat by the use of suitable plastic strip retainers.

Representative photographs of brass, stainless steel, and silicon are presented in Figs. 9, 10, and 11, respectively. All photographs reveal the same characteristic dot discharge pattern with relatively uniform dot spacing. The general trends noted in this study were the following:

(i) For a given electrode material, increased pulse width increased the dot intensity [see Fig. 9(b) compared to 9(a)].

(ii) For a given pulse width and electrode material, multiple pulses resulted in a descrease in the average interdot spacing [see Figs. 10(a), 10(c), and 11(a) compared to Figs. 10(b), 10(d), and 11(b), respectively].

(iii) For a given pulse width and approximately constant electrode spacing, the interdot spacing λ varies only slightly with material. Since the interdot spacing is a strong function of electrode spacing, any differences in interdot spacing for different materials may well be accounted for by a slightly different electrode spacing for the three materials.

(iv) For a given material, increasing electrode spacing results in less discrete dots (dot clustering) and an increase in the amount of diffuse exposure around each dot [see Figs. 9(c) and 11(c) compared to Figs. 9(b) and 11(a), respectively].

(v) For laterally displaced electrodes (relative to each other) giving only a fractional area of electrode overlap, the shape of the discharge not only conforms to the shape of the overlap area but one sees an additional edge discharge from the upper edge that overlies the metal on the lower electrode [see Fig. 9(d)].

(vi) In a number of photographs, large clear patches containing no dots were found [see Figs. 9(e), 9(f), 11(d), and 11(e) compared to Figs. 9(b), 9(d), 11(a), and 11(a), respectively].

As an attempt to evaluate the effect different materials have on the discharge while, at the same time, eliminating some of the problems associated with nonidentical test conditions, we constructed a composite circular electrode from a silicon wafer sputtered with a 3000-Å layer of platinum over the entire surface followed by a 3000-Å layer of zinc over half of the surface (one semicircular region). In Fig. 12, one sees the usual dot pattern from this composite (Pt-Zn) electrode with very little difference in interdot spacing λ between the two materials in spite of the fact that the work function differed by ~2 V. One does see an increase in the background exposure for the Pt which is probably due to the greater reflectivity of the Pt surface.

IV. DISCUSSION

One has only to casually read the work of Loeb[4] to realize that we are dealing here with the corona discharge phenomenon called "streamers". The various states in the development of streamers[4–10] begin with electrons being released from the cathode by natural ionizing events (cosmic rays) or uv radiation, or field emission. These electrons are accelerated by the field and ionize the air molecules yielding an exponential growth in the number of electrons and positive ions, i.e., an avalanche. The electrons, owing to their small mass, drift at velocities ~200 times that of the positive ions and are quickly swept to the anode. The electron avalanche releases photons from the anode which produces

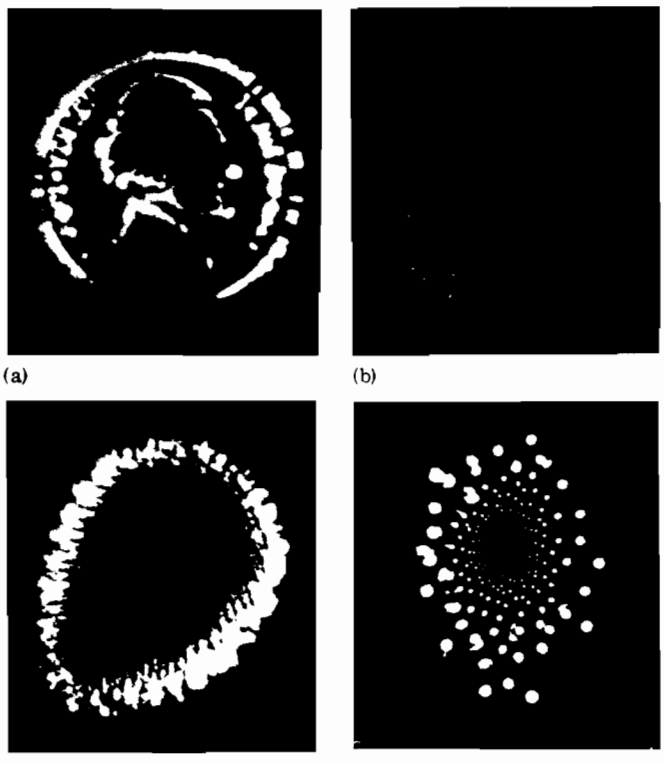

FIG. 6. (a) Photograph of coin (U.S. nickel); multiple pulses, pulse width = 100 μsec, rep. rate = 20 Hz, duration ~ 2 sec (1.7×). (b) Photograph of coin (U.S. nickel); single pulse, pulse width = 100 μsec, rep. rate = 1 Hz (1.7×). (c) Photograph of fingertip; multiple pulses, pulse width = 100 μsec, rep. rate = 20 Hz, duration ~ 2 sec (3.5×). (d) Photograph of fingertip; single pulse, pulse width = 100 μsec, rep. rate = 1 Hz (2.6×).

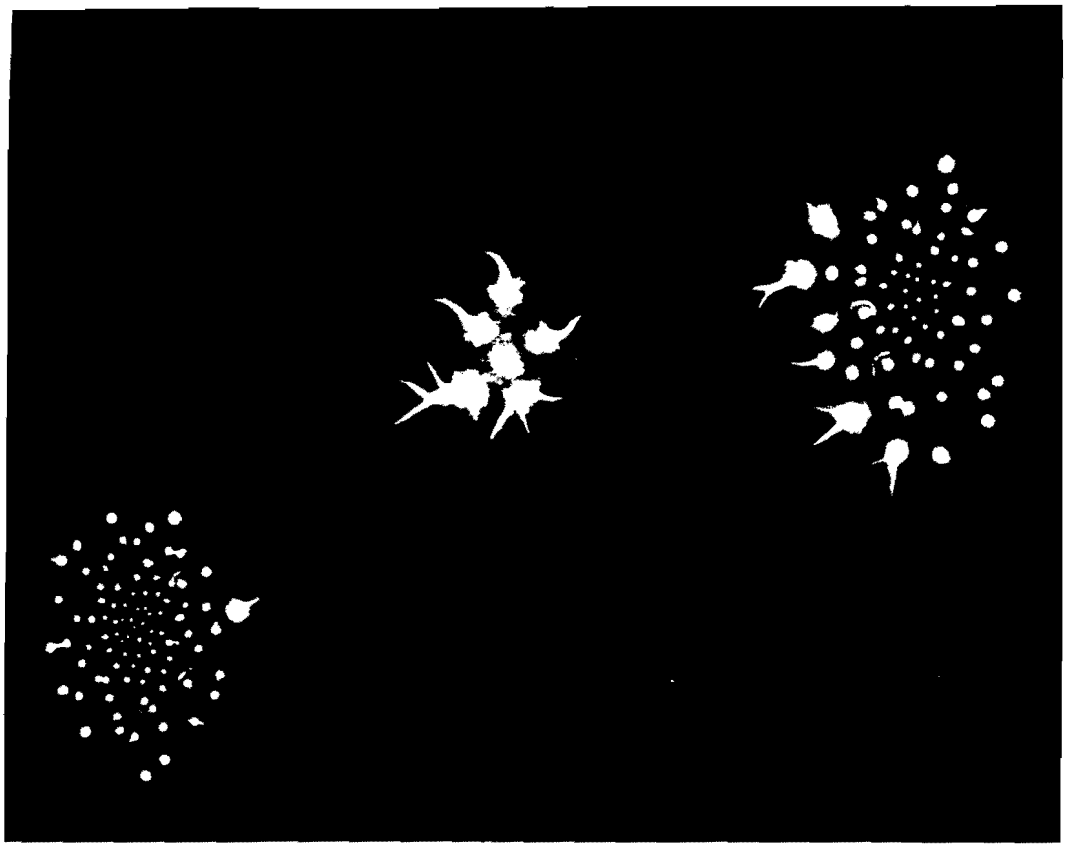

FIG. 7. Photograph of fingertip for different spacing between finger at electrode-film surface. Pulse width = 100 μsec, single pulse. Discharge space d is largest for center photo (3×).

additional local ionization of the air. At threshold voltage or above, an avalanche of positive ions, which often becomes a positive streamer, moves toward the cathode at high speeds (~10^7—10^8 cm/sec). The high-potential tips of the streamers are luminous and about 0.007 cm in diameter. As such a high-potential front approaches the cathode, tremendous fields are built up and the intense uv light from the luminous tip creates a burst of photoelectrons to be ejected from the cathode. These multiply rapidly in the high field, leading to an intensely ionized and accelerating high-field region that propagates itself to the anode as a potential space wave of ionization at extremely high speeds.[4] Thus, a ready mechanism exists to produce both positive and negative streamers moving between the electrodes. These branch at sufficiently high potentials to give rise to the beautiful Lichtenberg figures studied by Nasser.[5] In air, at high field strengths, the normal color of the streamers is a bright blue, since the most frequently excited radiation is from the second positive band group of highly excited N_2 molecules. Thus, if one was to visually observe the streamer propagation in the interelectrode space, he would see a group of discrete "balls of light", "light globules", or "light pulses" moving in various directions (depending on electrode shape) and leaving a dark interval behind once they passed in any direction. In air, at low electric fields, the ionization and excitation favor the arc spectrum of N_2 and nitric oxide yielding a reddish-purple glow. Yellow flashes have sometimes been observed in the streamer corona and this is thought to be due to the presence of Na from NaCl on the electrode surface. In addition, it is thought that if minute carbon flakes are ejected from the electrodes and rendered incandescent in the corona bursts, these could give rise to red or yellow streaks of light. However, a bluish-white color is the overwhelmingly dominant feature of the discharge.

The work of this paper differs from much of the earlier

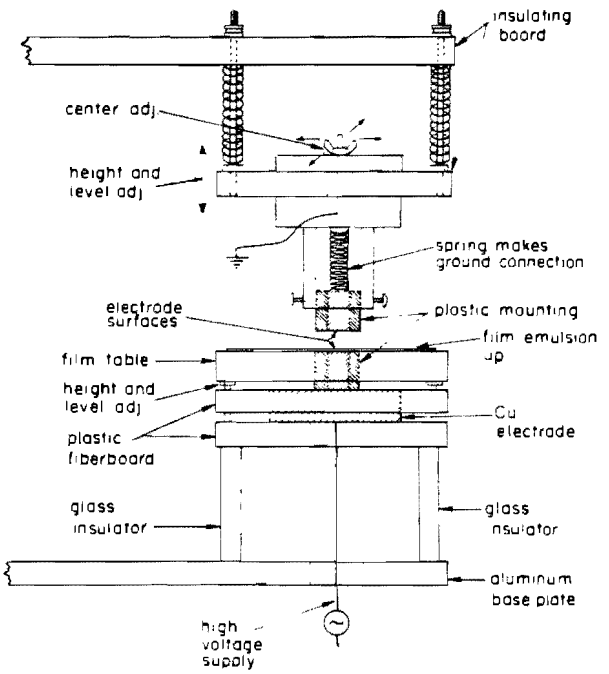

FIG. 8. Electrode holder for polished metal electrodes. Electrodes are fixed in a plastic mounting and placed in a parallel configuration in the apparatus, as shown.

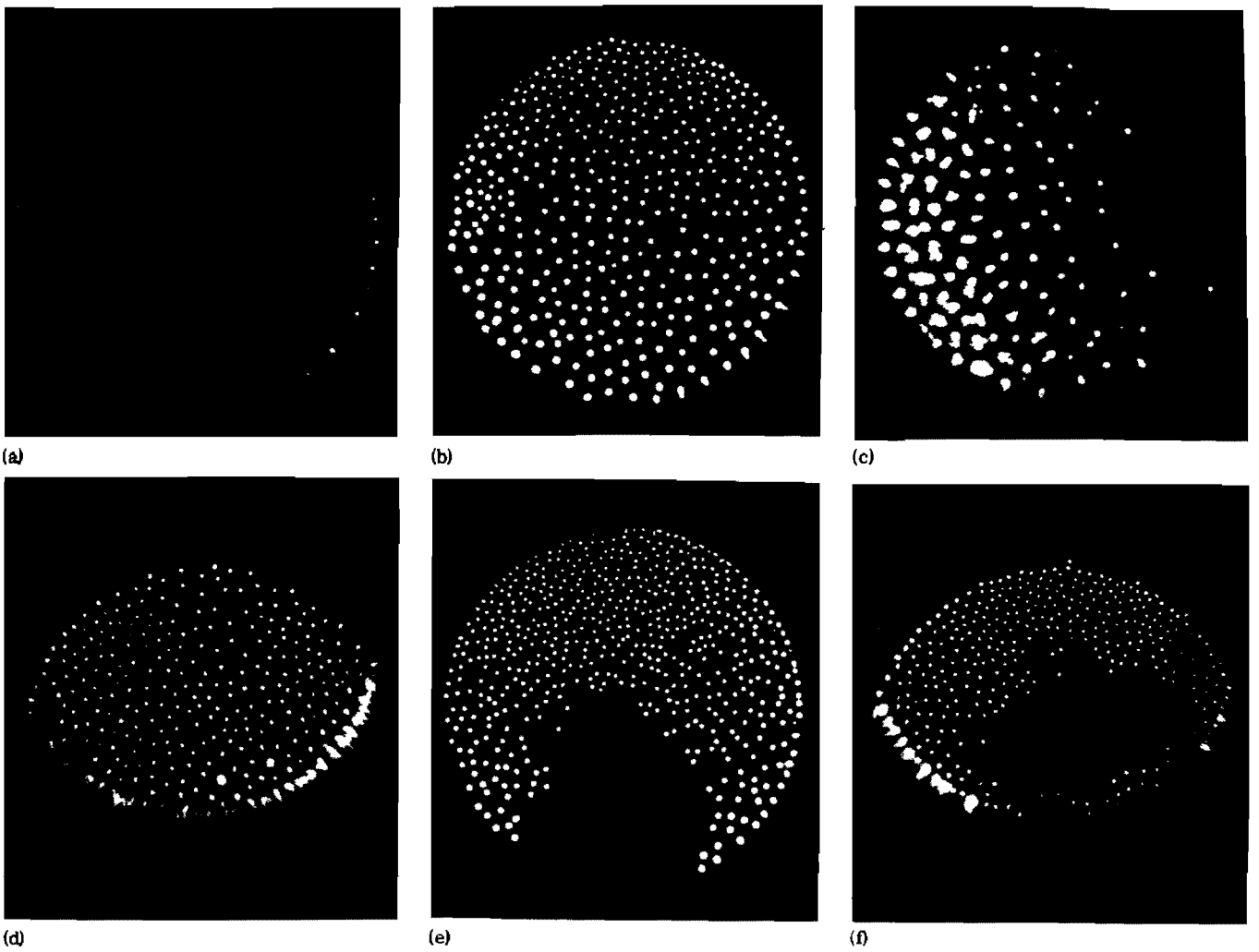

FIG. 9. Photographs of single-pulse discharge between flat polished brass electrodes under conditions of different pulse exposure, electrode spacing, and orientation (3.5×). (a) Pulse width = 100 μsec. (b) Pulse width = 500 μsec. (c) Pulse width = 500 μsec; nonparallel d, slight increase in discharge spacing d. (d) Pulse width = 500 μsec; electrode areas nonconcentric. (e) Pulse width = 500 μsec; local film buckling. (f) Pulse width = 500 μsec; local film buckling for nonconcentric areas.

work of Nasser for point-to-plane discharges[5] in that the electrode configuration is different; the interelectrode spacing is 1—2 orders of magnitude smaller. However, the applied fields in this study are equal to those applied at the point in the point-to-plane corona discharge studies for 0.25-mm radii ($E \approx 10^6$ V/cm and $V \approx 2 \times 10^4$ V). We have used pulsed rf, whereas the corona discharge work was done with pulsed dc. In addition, our interest has been on the effect of electrode material on the process. Certainly, from the reported streamer velocity,[4] our electrode spacing, and frequency of voltage oscillations, streamers could readily cross between the electrodes in every half-cycle. If photoelectron emission from the cathode is the key process for negative streamer formation, then one can readily understand the presence of only a small work-function effect for different metals, since the natural photon energy $h\nu$ is probably greater than that needed for electron emission for any metal under these high-field conditions. However, for large-band-gap insulators and biological systems, the picture might be somewhat different (perhaps $h\nu - e^- + h\nu'$).

The main observation of this paper, i.e., the array of discharge dots, seems to be quite new and probably arises as a result of the electrode geometry and spacing. The dots probably represent streamer paths (positive and negative streamers move along the same track) and, since they are of the same basic charge nature, they would tend to repel each other by electrostatic repulsion. Since they are also fed by the diffusion of ions (created by photoionization) from the interstreamer space, we have a balance of forces which should lead to some optimum spacing λ, depending on the type of gas, pressure, voltage, etc., of the system. In addition, magnetic-pinch effects and surface-energy effects have an influence on λ.

We may hypothesize that the network of discharge points stays fixed during a single pulse because the points of emission occur from surface protuberances randomly located on the surface and, once firing, they keep firing. Longer pulse times should thus lead to greater exposure of the point network. With multiple pulses, time exists between pulses for ion recombination to

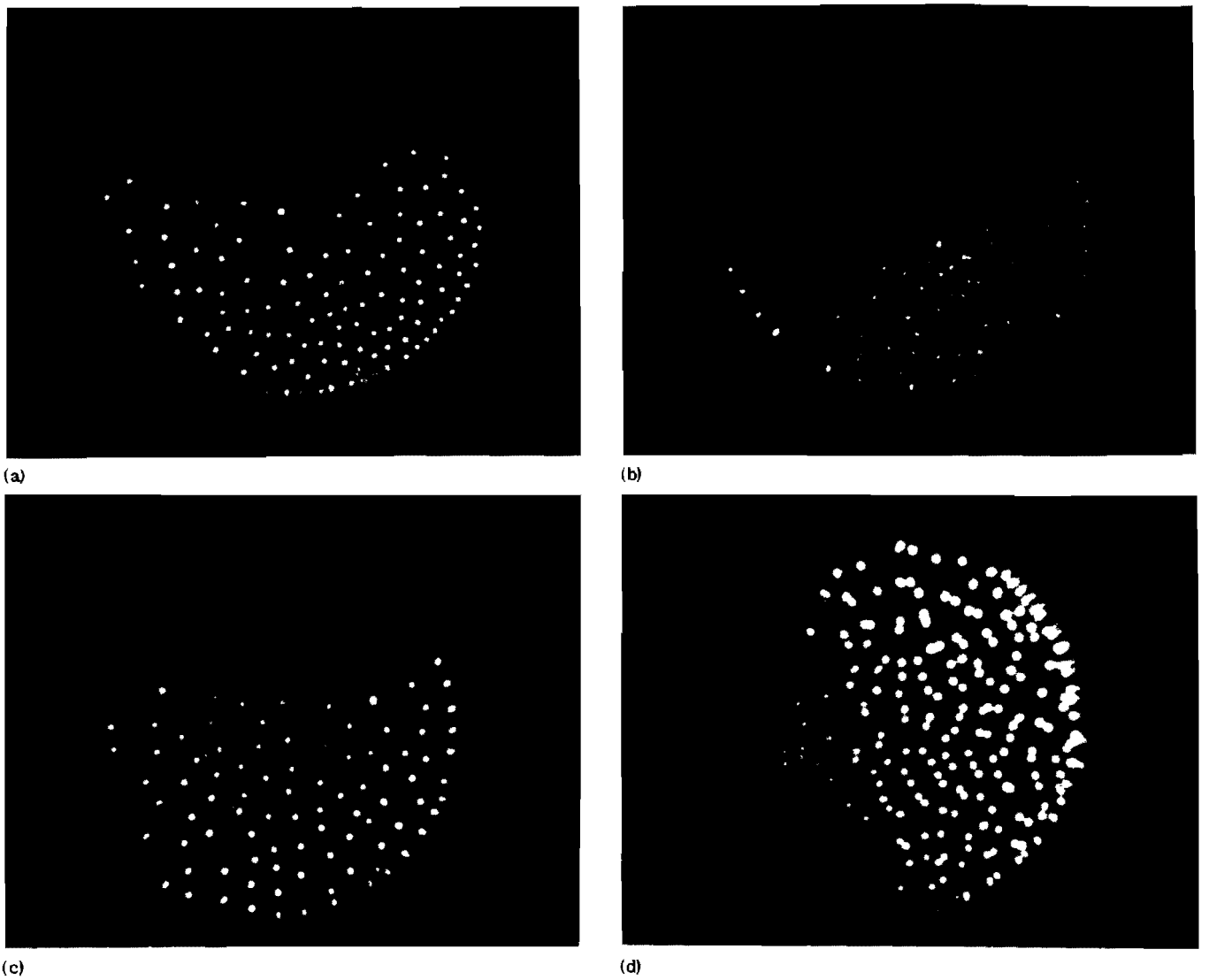

FIG. 10. Photographs of discharge between flat polished stainless-steel electrodes under conditions of different pulse exposure, electrode spacing, and orientation (3.7×). (a) Pulse width = 400 μsec and single pulse. (b) Pulse width = 200 μsec, rep. rate = 1 Hz, duration = 2 pulses. (c) Pulse width = 500 μsec, single pulse. (d) Pulse width = 500 μsec, rep. rate = 1 Hz, duration = 2 pulses.

occur and, thus, a new network of discharge points is expected to occur for each pulse.

Increasing the electrode spacing alters the field strength and, thus, both the electron impact ionization process and the photoionization process. Both of these effects could play a role in the discharge dot clustering.

The lack of dot discharge exposure over the entire electrode area may arise as a result of buckling of the film surface, resulting in a negligible discharge space over a specific patch of the electrode. Initial studies show that, when rigid glass photographic plates are used, the patch effect disappears.

From the fingertip studies, we seem to be dealing with the same basic process as with the polished metal electrodes. Thus, to understand the different colors and energy patterns associated with emission from living systems, we must begin to think in terms of positive and negative corona streamers passing between the electrodes and their consequences on film exposure. The available information inherent in the system can be divided into the two categories: (a) structure or shape features and (b) color features. Loeb[4] discusses some of the structure aspects indicating how the Lichtenberg figure pattern on the film changes with the separation distance between the film and electrode, applied voltage, and chemical constitution of the gas (strong water vapor effect diminishing intensity and sharpness of the pattern). Although circular blobs are a characteristic photographic form of the negative streamers and starlike or angular patterns are a characteristic photographic form for positive streamers, more work needs to be done to distinquish the structure differences associated with positive and negative streamers.

The work of Loeb[4] also discusses observations that allow us to consider the color aspect from a new point of view. Studies are described wherein a sheet of color film is exposed to streamers via (a) the emulsion side and (b) the nonemulsion side. In (a) the discharge patterns were found to be blue whereas in (b) they were red; i.e., the blue light and uv light entering via the backside of the film lead to a red imprint. To fully un-

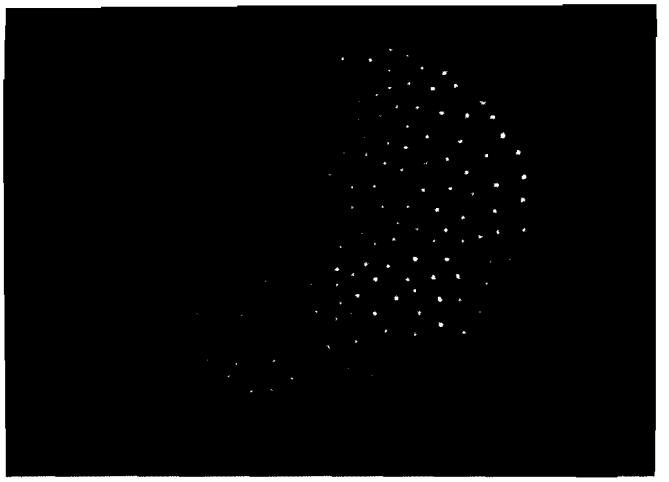

(a)

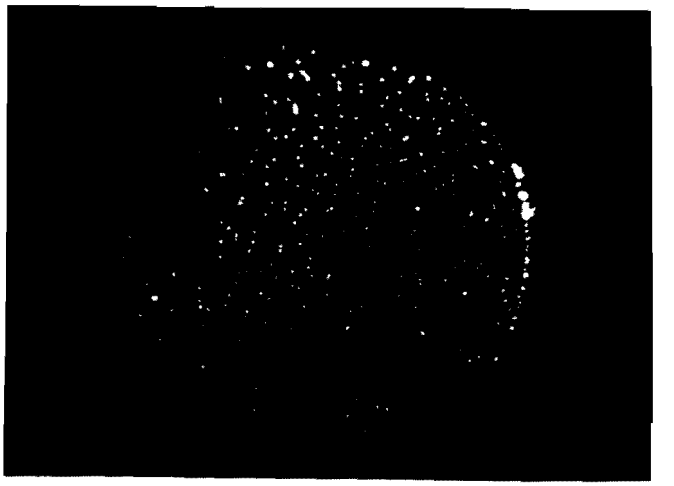

(b)

(c)

(d)

(e)

FIG. 11. Photographs of discharge between flat polished silicon electrodes under conditions of different pulse exposure, electrode spacing, and orientation (3.7×). (a) Pulse width = 500 μsec, single pulse. (b) Pulse width = 500 μsec, rep. rate = 1 Hz, duration = 2 pulses. (c) Pulse width = 500 μsec, single pulse; slight increase in discharge spacing d. (d) Pulse width = 500 μsec, single pulse, local film buckling. (e) Pulse width = 500 μsec, single pulse, local film buckling.

derstand this effect and to see its possible relationship to Kirlian photography, we must consider the layer construction of typical color film (see Fig. 13).[11–13]

The color film consists, essentially, of three emulsion layers separated by two filter layers and a plastic support or backing which is usually coated with a grey antihalation coating.[11–13] When white and uv light impinge on the film from the emulsion side, the first emulsion, a blue-sensitive film responding to uv and blue light, is exposed by the uv and blue components. The first filter layer passes the red and green components and the green component exposes the second emulsion, an orthochromatic emulsion sensitive to uv blue, and green. The second filter layer, which passes red and blue, allows the red component to pass and expose the third emul-

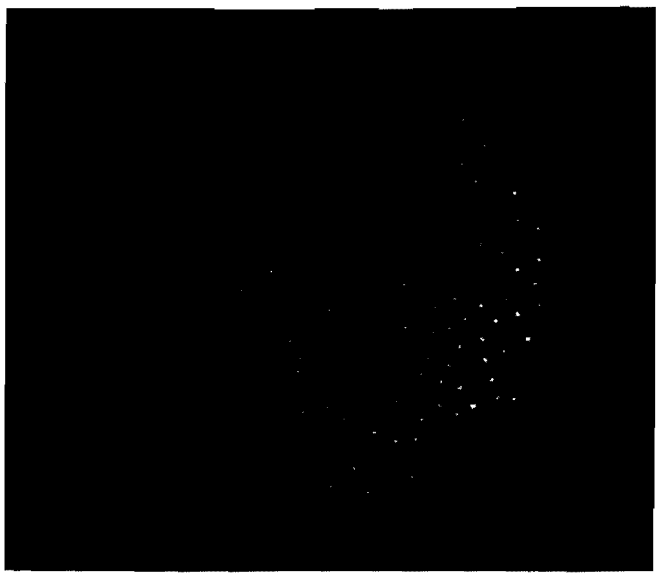

FIG. 12. Photograph of composite circular electrode—lower half-circle sputtered with zinc and upper half-circle sputtered with platinum (3.7×). Pulse width = 500 μsec, single pulse.

sion, a panchromatic emulsion sensitive to uv, blue, green, and red. Thus, the first emulsion is exposed by uv and blue, the second emulsion is exposed by green, and the third emulsion is exposed by red. Any attenuation of the red and green components due to passage through emulsion and filter layers is probably compensated for by making the second and third emulsions correspondingly more sensitive.

When white and uv light impinges on the film from the support side, the situation is quite different. The third emulsion (coding red) is exposed by all the light components. The second emulsion (coding green) is exposed by the blue component and the first emulsion (coding blue) remains unexposed (see Fig. 13). The resulting exposure would be a color mixture of red and green, which yields yellow for equal intensities. However, it is to be expected that the red layer will receive a much greater exposure than the green layer, yielding an overall result of orange or reddish orange. This effect is enhanced even further by the differing sensitivity of the two layers which have been adjusted to deal with light impinging on the film from the emulsion side. A very similar situation exists when only blue and uv light impinges on the film from the support side. However, because of the absence of a red component in the incident light, the composite color effect will be more towards the orange than towards the red, as in the general case of incident white light. A more accurate film model has a third emulsion sensitive to only red, blue, and uv. The insensitivity to green eliminated the need for a second filter layer. In our model, this alters the results only for the case of uv and green light entering the film from the support side providing yellow and green colors, respectively, instead of enhancing the red.

Let us now consider the effect of different spacings between the film and the adjacent electrodes. Imagine that we have placed a film, emulsion side up, in the device of Fig. 2 or Fig. 8 and have located it with the emulsion surface at distance d_1 from the upper electrode and the film support surface at distance d_2 from the lower electrode. Let both electrodes be of the same material. If $d_1 \approx d_2 \neq 0$, both positive and negative streamers bombard both sides of the film and, for only blue and uv light generated by the streamers, color film will show both red and blue patterns. If $d_2 = 0$, $d_1 \neq 0$ so that the film is firmly placed against the lower electrode, no streamers can develop on the support side of the film and the color film will show only blue patterns. Conversely, if $d_1 = 0$, $d_2 \neq 0$ so that the emulsion is firmly placed against the upper electrode, no streamers can develop on the emulsion side of the film, so the color film will show only reddish-orange patterns.

Since we are always using small electrode spacings ($d_1 + d_2 \sim 200$ μ), unless very great care is exercised, undulations in the film occur so that d_1 and d_2 vary over the surface of the film, resulting in some regions where the exposure is predominantly blue, some where it is predominantly reddish orange, and some of an intermediate hue. This is illustrated in Fig. 14. Our

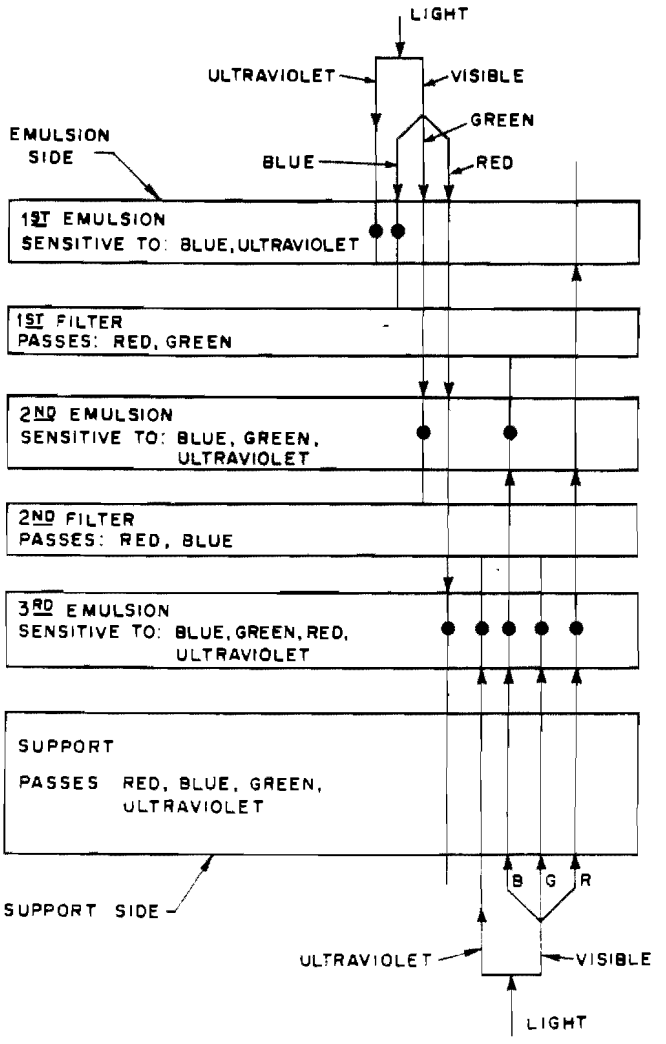

FIG. 13. Color film construction, a schematic representation of the effect of uv and visible light exposing the film from the emulsion side vs from the support side. Dot in light path indicates exposure of emulsion. (Note that the film actually uses a subtractive color system of yellow, magenta, and cyan. See Ref. 11.)

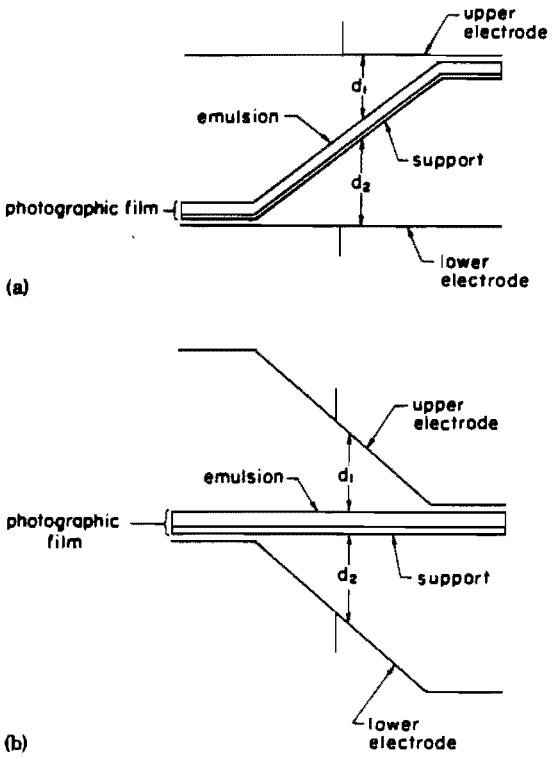

FIG. 14. Representation of film bending shown in exaggerated scale. (a) Film bent, electrodes planar; film exposure from left to right will be blue, white (blue, red, green), and orange (red, green), respectively. (b) Equivalent topological configuration to that in (a), except the electrodes are bent and the film is planar. All intermediate combinations at (a) and (b) are possible.

results, indicating blank patches among the dots when using film but none when using rigid glass plates, support the film distortion hypothesis. Because of these shape distortion effects, one must also expect the information pattern imprinted on the film to vary from place to place because, as Nasser showed,[5] the Lichtenberg patterns and intensity recorded on his film are a function of film location in the interelectrode gap.

Two other features that must be coped with are the asymmetrical electrode situation and the heterogeneous electrode situation. In the first case, one may be dealing with a metal electrode and a fingertip or leaf electrode, i.e., dissimilar materials. The fingertip or leaf electrode may not be effective in the generation of negative streamers so that, although one side is exposed to both positive and negative streamers, the other side is exposed to only positive streamers and, in different colors, different patterns may be recorded on the film. We anticipate that a biological surface is a heterogeneous electrode in that the work function of the surface for electron emission varies with position over the surface.[2] Such an effect will lead to a spatially specific location for streamer generation and, thus, a spatially varying intensity effect of the different color components (these may come from the electrode if the work function is sufficiently large and if $h\nu = e^- + h\nu'$).

Because of the foregoing, in this type of photography, one should paint the support side of the film with an

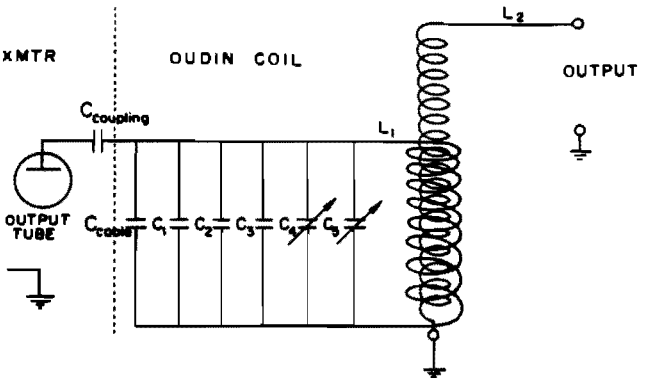

FIG. 15. Schematic of Oudin coil. (Explanation of symbols: C_C = 100 pF = coaxial cable capacitance; $C_{coupling}$ = 500 pF, 5 kV; C_1 = 500 pF, 5 kV; C_2 = 500 pF, 5 kV; C_3 = 100 pF, 5 kV; C_4 = 23—98 pF, 7 kV; C_5 = 23—98 pF, 7 kV; L_1 = primary coil, 15 turns, $\frac{3}{16}$-in.-diam copper tubing, 5 in. diam, 5 in. long, supported by Lucite supports; and L_2 = secondary coil, 500 turns, 24 AWG enameled wire, $3\frac{1}{4}$ in. diam, 10 in. long, wound on fiber board tube 12 in. long.

optically opaque coating and attach it firmly to a rigid support so that the emulsion-electrode spacing is constant everywhere on the film. Only then can one gather reliable information about electrode emission processes. This is consistent with the observation that, if one uses Polaroid color film, only blue and white pictures are observed; i.e., never any red or orange. In this case, the film backing is opaque.

We would anticipate that, if regular color film is turned over for a given film-electrode configuration, the color patterns should reverse, i.e., blue to red, etc. We also anticipate that, if film is not used and if a transparent electrode[2] is substituted, one will generally see only a blue-white pattern. However, if for living biological electrodes one sees different color manifestations, then these are probably associated with photoelectron emission from different energy states of the electrode.

In conclusion, we should note that although it now seems possible to account for the majority of the strange color effects observed in Kirlian photography, one cannot be certain that this is the only or the proper explanation. The results presented here illustrate that future Kirlian photography experiments must be done more carefully than those in the past, if we are to use this as a tool to learn truly new information about changes in energy states of living systems. Certainly the standard ionic processes discussed by Loeb[4] and others[5–10] are involved here and it is probably more appropriate to use the name "corona-discharge photography". Whether or not other new energies are also involved must be determined by the careful experiments of the future.

ACKNOWLEDGMENTS

The authors would like to acknowledge the helpful assistance of Dr. D. Clark in the design and construction of the high-voltage source. This research was sponsored by the Air Force Office of Scientific Research, Air Force Systems Command, USAF.

APPENDIX: rf SOURCE DETAILS

Figure 3 presents a block diagram of the high-voltage rf source. A sine-wave generator provides a 1-MHz signal (1—2 V rms) which drives a modified 6146B transmitter[14] through a tuned resonant circuit consisting of C_1, L_1, and L_2 (see transmitter schematic). The pulse generator drives the transmitter keying circuit (modified to include a transistor switch) with a 1—2 V 100 μsec—1 msec pulse, resulting in a keyed or pulsed sine-wave transmitter output. The pulse generator provides repetitive pulse output or, more typically, is externally triggered to provide a single pulse output. The transmitter output (~1500 V peak to peak) of pulsed rf from the plate of the output tube is coupled to the input of the Oudin coil through a suitable coupling capacitance and shielded coaxial cable.

In Fig. 15, the design of the Oudin coil is detailed where C_{cable}, C_1, C_2, C_3, C_4, C_5, and L_1 form a resonant circuit which is also tuned to 1 MHz. At resonance, the large circulating current induces a high voltage into the secondary circuit consisting of L_2 and the load. The voltage stepup would be given by the turns ratio in the ideal case; however, it is somewhat less in the real case of loose coupling, leakage, and losses.

[1] S. Ostrander and L. Schroeder *Psychic Discoveries behind the Iron Curtain* (Prentice-Hall, New York, 1970).
[2] W. A. Tiller, *Proceedings of the First Western Hemisphere Conference on Kirlian Photography, Acupuncture and the Human Aura*, May, 1972 (Gordon and Breach, New York, 1973).
[3] T. Moss and K. Johnson, Psychic Magazine, July (1972).
[4] L. B. Loeb, *Electrical Coronas—Their Basic Physical Mechanisms* (University of California Press, Berkeley, California, 1965).
[5] E. Nasser and L. B. Loeb, J. Appl. Phys. **34**, 3340 (1963).
[6] E. Kuffel and M. Abdullah, *High Voltage Engineering* (Pergamon, New York, 1970).
[7] H. W. Bandel, Phys. Rev. **84**, 92 (1951).
[8] G. A. Dawson and W. P. Winn, Z. Phys. **183**, 159 (1965).
[9] G. A. Dawson, Z. Phys. **183**, 172 (1965).
[10] L. E. Reukema, Trans. Am. Inst. Electr. Eng. **47**, 38 (1928).
[11] D. A. Spencer, *Color Photography in Practice* (Focal Press, New York, 1966).
[12] Kodak Color Films, Kodak Data Book No. E-77, 1971.
[13] Kodak Professional Black and White Films, Kodak Data Book No. E-5.
[14] 6146B Transmitter—A 75-120 Watt 6146B Transmitter, *The Radio Amateur's Handbook*, 42nd ed. (Byron Goodman, New York, 1965).